Long-term Culturing of *Pseudomonas aeruginosa* in Static, Minimal Nutrient Medium Results in Increased Pyocyanin Production, Reduced Biofilm Production, and Loss of Motility

Rhiannon Cecil[1], Elana Ornelas[1], Anh Phan[1], Deborah Yoder-Himes[1]

[1] Department of Biology, University of Louisville, Louisville, KY, U.S.A. 40292

Abstract:

Pseudomonas aeruginosa is a multidrug-resistant opportunistic human pathogen that can survive in many natural and anthropogenic environments. It is a leading cause of morbidity in individuals with cystic fibrosis and is one of the most prevalent pathogens associated with nosocomial infections in the United States. It has been shown that this organism can survive and persist in low nutrient environments such as sink drains and inside the respiratory system of human hosts. How adaptation to these types of environments influences phenotypic traits of this organism has not been well studied. Here we implemented an experimental evolution system designed to imitate these environmental niches and identified phenotypic changes that occurred as a result of adaptation to such environments in six strains of *P. aeruginosa* with varying life history and colony phenotypes. We observed that adaptation to low nutrient environments resulted in decreased generation time, reduced cell size, reduced biofilm formation, increased pyocyanin production, and decreased motility. Our work is significant as it allows us to predict how this organism will evolve in hospital and domestic environments and can help us improve treatment options for patients.

Introduction:

Experimental evolution provides a powerful means of understanding fundamental evolutionary processes and can also be used to increase our understanding of how virulence factors in opportunistic pathogens arise or change over time [1, 2]. In this study, we sought to use an experimental evolution system to determine how an opportunistic human pathogen, *Pseudomonas aeruginosa*, adapts to a low nutrient, static environment over the course of approximately 2,000 generations. We sought to determine if adaptation to this type of environment would result in changes to phenotypes commonly associated with growth and/or pathogenicity. We also sought to determine if long-term culture in a low nutrient environment under static conditions would result in increased or decreased fitness against a phagocytic predator, *Acanthamoeba castellanii*, which would suggest that adaptation to such environments could result in increased virulence in other organisms. *A. castellanii* is a bacterivorous amoeba species which shares many conserved pathways and mechanism with human macrophage such as P_{21}-activated kinases (involved in cell motility, differentiation, and gene signaling), Ras (signaling) and Rab (vesicle fusion) proteins, PI phosphatases and PI kinases (cell signaling and phagocytosis), and mannose binding proteins (adhesion and activation of innate immune response) [3-6]. Thus, it provides a model system to better understand how evolved *P. aeruginosa* responds to phagocytic predators.

P. aeruginosa is a member of the ESKAPE group of bacterial pathogens [7]. It is a dangerous opportunistic pathogen due to its intrinsic multidrug resistance, genomic plasticity, ability to survive and form biofilms on abiotic surfaces such as hospital equipment, and ability to evade the immune systems of humans, plants, and non-human animals [8-12]. *P. aeruginosa* commonly

presents with three colony morphotypes: wild-type, small colony, and mucoid. The colony morphology of *P. aeruginosa* can be partly attributed to the amount of cyclic di-GMP (c-di-GMP) produced within the cell. c-di-GMP is a ubiquitous bacterial second messenger that functions as one of the global regulators in *P. aeruginosa* [13-15]. Low levels of c-di-GMP leads to *P. aeruginosa* with faster growth rates, larger colony sizes, flagellar motility, and is associated with a planktonic lifestyle and expression of virulence factors such as the Type 3 Secretion System (T3SS) [13, 16]. In contrast, high concentrations of c-di-GMP are typically seen in the small colony and mucoid phenotypes, which are associated with slow growth, increased biofilm formation, reduced motility, and reduced virulence [14, 16]. Typically *P. aeruginosa* isolated from environmental samples bear the wild-type "normal" colony morphology while *P. aeruginosa* from clinical samples taken during chronic human infections have the small colony or mucoid colony morphologies [17, 18].

P. aeruginosa is a well-studied organism; however, how it evolves when forced to adapt to a low-nutrient environment has not been thoroughly investigated. Understanding how *P. aeruginosa* adapts to survive in a low-nutrient medium under static conditions could increase our understanding of how *P. aeruginosa* adapts in other low nutrient environments including sink drains, intubation tubes and other types of hospital equipment, human tissues, and other such reservoirs where this organism is able to thrive. *P. aeruginosa* presents with a wide arsenal of phenotypes that serve as a means of offensive and defensive protection against competitors and predators in the environment (e.g., protozoa, nematodes) such as pyocyanin production, biofilm formation, and T3SS expression [19-21]. Many of these phenotypes coincidentally act as virulence factors should the bacterium encounter a human host. This work is significant as it provides a "sneak peek" into how *P. aeruginosa* virulence factors and non-virulence factor

phenotypes might change over time in similar environments such as sink drains and hospital equipment and whether these changes could result in increased virulence in a model system.

Materials and Methods

Bacterial strains and culture maintenance

P. aeruginosa strains used in this study were chosen based on their colony phenotype, pyocin profile, and source of isolation. Strain details are listed in Table 1 and their respective pyocin profiles are shown in Table 2. Cells were routinely maintained on LB (Lennox) agar plates at room temperature (22°C) or grown in LB (Lennox) broth. Prior to initiation of an experiment, a single colony would be transferred from a LB agar plate to either glass test tubes containing 5 mL of LB broth, 96-well deep plates containing 1% HL5 medium (Formedium, HLG0102), or 96-well polystyrene plates containing 180 µL of LB broth and incubated overnight at 37°C with or without aeration as indicated. When indicated, mid-log cultures were generated from overnight liquid culture by transferring 100 µL of overnight culture to 5 mL of sterile LB broth and incubated at 37°C with aeration for 90 minutes.

Experimental Evolution Methods

Each strain was cultured in 8 mL of 1% HL5 in 6-well tissue culture plates. The plates were incubated at room temperature under static conditions. Every 2 to 3 days the medium was removed with vacuum suction and replaced with 8 mL of fresh sterile 1% HL5 medium. The evolving populations were also passaged every 7 days by removing the supernatant, adding 4 mL

of sterile 1% HL5, scraped with a cell scraper to dislodge the adherent cells. The suspended cells were transferred to a sterile 15 mL conical tube and centrifuged at 6,976 x *g* for 15 minutes at room temperature. The pellets were resuspended in 1 mL of 1% HL5 and 500 µl was added to 8 mL of sterile 1% HL5 in fresh 6-well tissue culture plates. A strain collection was generated at bi-weekly time points by transferring 500 µL of culture to 500 µL of sterile LB+40% glycerol (glycerol 20% final concentration) with subsequent storage at -80°C. At each dilution step, lineages were tested for contamination via colony PCR for pyocin genes. Pyocins are proteins exclusively produced by *P. aeruginosa*. The pyocin profiles were used to ensure that no cross contamination occurred between the strains throughout the experimental evolution via colony PCR using primers for the specific pyocin genes as in [22]. Lineages were evolved for 12 weeks total time.

Generation time

Overnight cultures of ancestral and evolved isolates were grown in 1 mL of 1% HL5 in 96-well deep plates with aeration at 30°C. The following day 5 µl of overnight culture was transferred to a 96-well dilution plate containing 175 µL of 1% HL5. The lid was placed on the plate and parafilm was used to seal around the edges of the lid to prevent liquid escape. The plates were incubated at room temperature for 48 hours in a 96-well spectrophotometer (Molecular Devices). The spectrophotometer measured the optical density of the wells every 30 minutes and was set to shake the plate for 5 seconds to resuspend cells prior to each read.

Cell Size

Overnight cultures of ancestral and evolved isolates were generated in 5 mL of LB broth in glass test tubes with aeration. 20 µL of overnight culture was transferred onto a glass microscope slide along with a drop of 1% congo red staining solution. The mixture was smeared across the slide then allowed to dry for 5 minutes in a biosafety cabinet. The slides were viewed under a light microscope with an ocular micrometer to measure the length of 20 individual cells from each ancestral and evolved lineage.

Biofilm biomass quantification

Biofilms were quantitated via a slightly modified version of a previously published protocol [23]. Briefly, overnight cultures of ancestral and evolved lineages in replicates of four of each isolate were generated in 180 µL of LB in 96-well dilution plates without aeration. Biofilms were set-up by first using a 96-well transfer apparatus to transfer inocula of overnight culture to fresh 96-well PVC plates containing 100 µL of 1% HL5. The inoculated plates were sealed with porous adhesive film (VWR, 60941-086), loosely wrapped with aluminum foil, and then placed in a humidity chamber with sterile water at the bottom. The lid of the humidity chamber was loosely sealed to allow for air flow while also maintaining a moist environment. The plates were incubated at 37°C for 24 hours to allow for biofilm formation. After 24 hours the biofilms were washed two times with water then 125 µL of 0.1% crystal violet was added to each well and the plates were allowed to incubate at room temperature for 10 minutes. Afterwards, the biofilms were washed four more times with water. Then 200 µL of 30% acetic acid solution was added to each well and allowed to incubate at room temperature for 15

minutes. A 96-well plate reader was used to quantify crystal violet in solution at an optical density of 500 nm.

Pyocyanin and pyoverdine production

Pigment levels from *P. aeruginosa* strains were determined using protocols modified from a previously published study [24]. Overnight cultures were generated in 5 mL of LB broth with aeration in glass test tubes. 100 µL of overnight culture was transferred to 1 mL of LB broth in 24-well plates. The plates were sealed with porous adhesive film (VWR, 60941-086) and incubated at 37°C for 48 hours under static conditions. Post-incubation, 1 mL of each sample was transferred from the 24-well plates to 1.5 mL microfuge tubes. The tubes were then centrifuged at 21,130 x *g* for 30 minutes to pellet the bacteria, and 100 µL of supernatant from each culture was transferred to either 96-well clear plates (VWR, #10861-562) for pyocyanin quantitation or 96-well black plates (Greiner, #655077) for pyoverdine. A 96-well plate reader was used to quantify the amount of pyocyanin (absorbance at 686 nm) or pyoverdine (fluorescence 395ex/460em).

Motility assays

The motility protocol used in this study was modified from the motility assay described in [24]. Overnight cultures of ancestral and evolved isolates (each n = 3) were grown in 5 mL of LB broth in glass test tubes with aeration. Briefly, a 2 – 10 µL pipet tip was dipped in overnight culture then was used to stab approximately half-way deep into the motility agar (10 mL of 0.3%

LB agar in 6-well plates). The inoculated plates were incubated at room temperature for 24 hours. The diameter of spread was measured using a metric ruler to quantify swimming distance.

Acanthamoeba castellanii culture and maintenance

A. castellanii cells were routinely maintained at room temperature in T-75 tissue culture flasks containing 15 mL of 100% HL5 growth medium. The cells were passaged routinely when they reached confluence, ~ every 3 days, using a cell scraper to dislodge the cells from the bottom of the flask, then removing all but 1 mL of culture from the flask and replacing with 14 mL of sterile 100% HL5. Cell stock cultures were maintained up to 4 passages.

Co-culture experiment with *Acanthamoeba castellanii*

After reaching confluence, approximately 6 x 10^3 *A. castellanii* cells, based on hemocytometer counts, were transferred to wells of 6-well tissue culture plates along with 4 mL of 100% HL5 medium. The cells were incubated at room temperature for 1 hour to allow the cells time to anneal to the surface of the wells in the 6-well tissue culture plates. The 4 mL of 100% HL5 was then removed, and the wells were washed 2 times with sterile 1X PBS then 8 mL of 1% HL5 was added to the wells. Overnight cultures of ancestral *P. aeruginosa* and one of the evolved lineages of each *P. aeruginosa* strain were generated in triplicate in 5 mL of LB broth. Mid-log cultures were generated as previously described above until an $O.D._{600}$ between 0.8 and 1.0 was reached for all strains. *P. aeruginosa* cells were added to the 6-well tissue culture plates in a ratio of 1 *P. aeruginosa* cell to 10 *A. castellanii* cells in 3 biological replicates per *P. aeruginosa* isolate.

The plates were incubated at room temperature for 16 days. Every three days the medium was replaced by using vacuum suction and replaced with 8 mL of sterile 1% HL5. *A. castellanii* cells were enumerated on days 0, 3, 6, 8, 11, 13, and 16 via direct cell count at 400X magnification. *P. aeruginosa* cells were enumerated on day 16 via serial dilution and plating on LB agar plates.

Statistics:

Data was analyzed with one-way ANOVA with Tukey's or Dunnett's post-test or with t-tests as described below in GraphPad Prism 5.0.4 as indicated.

Table 1: Strains used in study.

Strain	**Origin**	**Colony Phenotype**	**Reference**
PA B80398	Clinical – CF sputum	Normal Colony	[22]
PA B80427	Clinical – CF sputum	Small Colony	[22]
PA B84725	Clinical – CF sputum	Mucoid	[22]
PA3	Clinical – CF sputum	Normal Colony	[22]
SRP 17-047	Environmental – Bathroom sink drain	Normal Colony	[25-27]
SRP 17-055	Environmental – Kitchen sink drain	Normal Colony	[25-27]

Table 2: Pyocin profile of strains used in study.

Strain	**S1-type** [a]	**S2-type**	**S1S2 immunity**	**R-type**	**F-type**
PA B80398	1	0	0	1	0

PA B80427	0	1	1	1	1
PA B84725	0	0	0	1	1
PA3	0	1	0	1	0
SRP 17-047	1	0	1	1	0
SRP 17-055	1	0	1	1	1

[a]1 indicates presence of the pyocin gene in the genome, 0 indicates absent from the genome.

Results:

To test how a variety of *P. aeruginosa* phenotypes change in response to forced growth in a low-nutrient environment, we conducted a 12-week-long experimental evolution on six *P. aeruginosa* strains. Four of these strains were of clinical origin (PA B80398, PA B80427, PA B84725, and PA3) and two strains were of environmental origin (SRP 17-047 and SRP 17-055) as they were isolated from household sink drains. These strains were chosen based on their colony phenotypes, pigment production, and pyocin profiles and these strains represent a wide range of *P. aeruginosa* morphotypes. Four of the strains (PA B80398, PA3, SRP 17-047, and SRP 17-055) present with "normal" colony morphology. The normal colony phenotype of *P. aeruginosa* is frequently isolated from acute infections or environmental samples and is associated with more aggressive virulence factors such as pyocyin production and Type 3 secretion systems as well as increased motility and a predisposition to planktonic lifestyle [13-15]. The other two strains (PA B80427 and PA B84725) are small colony and mucoid respectively, both of which are often isolated from chronic infections and are not known to be isolated from environmental samples. The small colony and mucoid phenotype commonly present with defensive virulence factors to avoid detection by the host's immune system such as

reduction in motility and increased biofilm formation [14, 16]. The mucoid phenotype also overproduces the carbohydrate polymer alginate making them difficult to phagocytose [28].

An experimental evolution was designed to mimic the conditions that *P. aeruginosa* would encounter in a non-host environment, such as the soil or an abiotic surface such as a sink drain. To mimic these environments, *P. aeruginosa* was cultured over time under static conditions (to encourage niche specialization) in a low nutrient medium (1% HL5). Every two days, the medium was removed via vacuum suction [simulating the flow of liquid down a sink drain (i.e. frequent mechanical removal)]. This removes most of the planktonic cells, thus selecting for cells that can attach to the surface of the wells. Every 7 days the medium was removed, and the adherent cells were scraped from the wells and diluted back into sterile 6-well tissue culture plates containing sterile 1% HL5. This process was continued for 12 weeks generating three biological replicate lineages of the six *P. aeruginosa* strains. To ensure that no contamination occurred along the way, lineages were routinely analyzed for pyocin gene profiles, which were distinct and specific for each strain, via PCR. The ancestral and evolved lineages were then tested for a variety of phenotypes associated with growth, long-term survival, or virulence. These phenotypes included generation time, cell size, biofilm formation, pyocyanin and pyoverdine production, and motility.

<u>Overall cellular changes during evolution in a low nutrient medium</u>

During evolution experiments, an increase in fitness of the evolved lineage compared to its ancestor usually occurs as the organisms adapt to their conditions. One global indicator of fitness in bacteria is generation time. A decreased generation time in 1% HL5 at room

temperature would indicate that the evolved isolates have an increased fitness in this environment compared to their ancestors and thus this measurement serves as a control for the experimental evolution. We assessed growth of all ancestral and representative isolates from evolved lines in 1% HL5 over time and calculated the relative generation time for each isolate. The data analysis was compiled in two ways. First, all lineages were grouped for a particular strain and condition to assess global patterns that might arise. Second, all the isolates together for each lineage were analyzed to assess differences in replicate lineages.

The evolved lineages of all but one strain exhibited significantly decreased generation times compared to their ancestors both when grouped together (Fig. 1) and when assessing the evolved lineages individually (Fig. S1). In contrast, the evolved isolates of the remaining clinical strain, B84725, had significantly slower generation times compared to the B84725 ancestor strain when grouped together (Fig. 1). Each individual replicate evolved lineage of B84725 the generation times were also slower than their ancestral strain; however, these did not reach statistical significance in individual comparisons (Fig. S1). We acknowledge that the calculated generation times for the evolved lineages and some of the ancestors are much faster than what is typically observed for *P. aeruginosa* (25 min to 1.5 hours) [29]. However, these generation times are present in other bacteria species including in *Pseudomonas* species [30]. The growth curves used to calculate the generation time data are provided in (Fig. S2). Taken together, this data suggests that most of the evolved lineages of most of the strains grow faster in 1% HL5 compared to their ancestors and, further, that there are observable global changes that occur in the evolved lineages over the 3 month time period.

Cells size is also linked to metabolic fitness as an increased surface volume ratio results in amplified nutrient diffusion into the cell resulting in increased metabolic efficiency, especially

in low nutrient conditions [31, 32]. We hypothesized that an overall decrease in cell size would be observed in the evolved isolates as the low-nutrient concentration of the growth medium would encourage a smaller cell size to increase metabolic efficiency. Five of the six strains showed a small reduction in cell size after the experimental evolution, of which three (clinical isolates, B80398 and B80427, and the environmental isolate, SRP 17-047) were significantly reduced compared to the ancestral strain (Figs. 2, S2). Curiously, the evolved lineages of PA3 increased significantly in size compared to the ancestor; however, this ancestral strain was relatively small to begin with, which might imply that PA3 was already adapted to lower nutrient conditions. Our cell size data overall suggests that, as expected, a reduction in cell size was selected for in low-nutrient environments for *P. aeruginosa*.

The first classic *P. aeruginosa* phenotype assessed was biofilm formation. Based on the design of our experimental evolution, we hypothesized that the evolved lineages would be superior biofilm formers compared to their ancestors because our experimental evolution design strongly selected for cells that were adhered to the tissue culture surface. We assessed biofilm formation with crystal violet assays which provide a broad quantitative means to assess the volume of biofilm biomass produced.

Surprisingly, only two strains, PA B80398 and PA3, exhibited significantly different biofilm densities compared to their ancestor strains (Fig. 3). In both instances, the evolved lineages exhibited significantly reduced biofilm biomass than their ancestors though the overall degree of loss is quite small. This result is consistent when considering each evolved lineage separately as all lineages showed reduced biofilm biomass (Fig. S3) which suggests that this change was not driven by data from a single lineage but likely represents a true shift in the phenotype for these strains. All the remaining evolved lineages tested were not significantly

different from their ancestor with respect to biofilm formation (Fig. 3 and S3). From these results, we conclude that biofilm formation was not selected for in our evolution experiment or that the conditions were inhospitable to biofilm formation. We suspect that attachment to the tissue-culture surface was likely achieved by some other means than formation of a biofilm as only attached cells were propagated in subsequent passages in the experiment.

Individual molecular phenotypes

Pyocyanin is a redox-active toxin secreted by *P. aeruginosa.* It is toxic to eukaryotic cells and provides *P. aeruginosa* protection against predators, but it also serves as a secondary metabolite for *P. aeruginosa* and is associated with promoting survival in low-oxygen and low-nutrient environments [33-35]. We hypothesized that the evolved lineages would produce significantly more pyocyanin than their ancestors due to the low-nutrient conditions present in our experimental evolution system. Our hypothesis was supported for three of the strains: PA B80427, SRP 17-047, and SRP 17-055, of which there was a small but significant increase in pyocyanin production in PA B80427 and SRP 17-047, and a large increase in SRP 17-055 (Fig. 4). Two strains, PA B80398 and PA B84725, did not exhibit significant differences in pyocyanin production compared to their ancestors; however, two of the individual evolved lineages of PA B80398 did produce more pyocyanin than their ancestor (Fig. S4). Interestingly, all three evolved lineages of PA3 produced significantly less pyocyanin compared to their ancestor suggesting that pyocyanin production was not selected for in this strain. The reasons for this remain unclear. From this data, it suggests that for most of our *P. aeruginosa* strains pyocyanin production was selected for in our experimental evolution system and increased pyocyanin increased the fitness of the organisms in these low nutrient environments.

Pyoverdine is a siderophore secreted by *P. aeruginosa* which functions to sequester iron from other cells as well as the environment [36]. The 1% HL5 used for the experimental evolution is undoubtedly low in most macronutrients. However, it likely does contain some iron as it contains yeast extract and protease peptone but whether the concentration was sufficient for *P. aeruginosa* growth is unknown. Therefore, we could not make a hypothesis on whether pyoverdine production would change over time in the evolved isolates. Pyoverdine is highly implicated in *P. aeruginosa* pathogenicity [37] so pyoverdine production was assessed using spectrophotometry in the ancestral and evolved lineages.

Pyoverdine remained unchanged in five of the six strains tested (Fig. 5). Only one of the evolved lineages of the environmental isolate, SRP 17-047 produced significantly less pyoverdine than its ancestor, while the other two lineages of 17-047 were not significantly different (Fig. S5). This suggests that pyoverdine was likely neither selected for nor against under the conditions in our experimental evolution system.

The last phenotype tested was swimming motility. We hypothesized that there would be a reduction in motility in our evolved lineages as our experimental evolution design selected against planktonic cells. The ancestral isolates had quite variable swimming abilities with one strain, the mucoid clinical isolate PA B84725, being completely amotile (Fig. 6). There was a significant reduction in swimming motility observed for almost all the evolved lineages compared to their ancestors for PA B80398, PA3, SRP 17-047, and SRP 17-055 after 12 weeks (Figs. 6A and S7). This is consistent when considering the evolved lineages individually as well, except for lineage 1 of SRP 17-047 (Fig. S7). The other two strains, PA B80427 and PA B84725, did not exhibit significant changes in motility compared to their ancestors; however, it is important to note that the ancestors for these two strains were either amotile (PA B84725), or

only weakly motile (PA B80427), under these conditions. Surprisingly, two of the evolved lineages, lines 1 and 3 of PA B80427, displayed small but significantly greater motility than the ancestor PA B80427 strain (Fig. S7).

We tested the earlier isolates of the four strains that lost motility over the course of the experiment (B80398, PA3, 17-047, and 17-055) to determine when motility was lost (Fig. 6B-E) by dynamically selecting time points, testing motility, and then altering either before or after to identify when motility was lost. We found that motility was lost at week 7 for two of the evolved lines of B80398 (Fig. 6B), week 5 for two lines of PA3 (Fig. 6C), week 2 for all three lines of the environmental strain 17-047 (Fig. 6D), and at 3 weeks for all three lines of 17-055 (Fig. 6E). Together these data suggest that for strains that were highly motile at the start of the experiment, motility was selected against and was lost between 2 and 7 weeks of culture in low-nutrient medium but that this varied for each motile strain.

Host-associated phenotypes over the course of evolution in a low nutrient environment

We also sought to determine if long-term adaptation to a low nutrient environment would result in an increased or decreased ability to survive and/or kill a phagocytic predator as this could be a strong indicator of how *P. aeruginosa* virulence can increase in low-nutrient environments. To test this, we co-cultured the ancestral isolates and one evolved lineage of each strain with the phagocytic amoeba species *A. castellanii* over time to examine the survival of both organisms. *A. castellanii*, is an avid predator of *P. aeruginosa* and is a model organism for studying phagocytosis [3-5, 38].

To first determine whether evolved isolates had an impact on trophozoite survival, we compiled the trophozoite survival in co-culture with all ancestral strains collectively over time and compared this to trophozoite survival in co-culture with all of the collective evolved lineages of each strain. The results revealed that trophozoite mortality was significantly greater when co-cultured with the evolved *P. aeruginosa* lineages compared to co-culture with the ancestral isolates ($p < 0.0001$) (Fig. 7). So overall, co-culture between amoebae and the evolved isolates tended to result in fewer living trophozoites compared to ancestral strains.

We then examined trophozoite and *P. aeruginosa* survival based on strains. By 16 days of co-culture, *A. castellanii* trophozoite survival was significantly reduced when co-cultured with the evolved lineages of the clinical isolates PA B80398 and PA3 than with the ancestral isolates of these strains (Fig. 8A). The remaining strains showed neither a statistical increase nor decrease in the number of trophozoites found, perhaps due to the large variability in the individual lineages. Trophozoite survival over time tended to be reduced when in co-culture with the evolved lineages compared to the ancestral strains (Fig. S8).

In comparison, all the *P. aeruginosa* isolates tested were able to survive in co-culture with *A. castellanii* for at least 16 days (Fig. 8B). There were no significant differences between the numbers of surviving evolved cells compared to ancestors at 16 days except for the clinical isolate, PA3, for which the number of surviving cells at 16 days was significantly greater for the evolved lineage than the ancestor (Fig. S8). Therefore, ancestral and evolved lineages of *P. aeruginosa* survived just fine in the presence of amoebae.

When looking at trophozoite survival over time in co-culture with the individual evolved lineages and their ancestors, in most instances the number of trophozoites were greater in co-culture with the ancestors than when co-cultured with the evolved isolates (Fig S8A – F).

However, the difference in trophozoite survival with the evolved lineages compared to ancestors was rarely significant (Fig S8A – F). *P. aeruginosa* cells were only enumerated on day 16 as we were able to confirm the presence of live *P. aeruginosa* cells in the wells using bright-field microscopy at each of the other time points. Based on the results of these data, we conclude that adaptations to a low nutrient environment under static conditions significantly increased virulence in *P. aeruginosa* against a phagocytic predator; it also did not adversely affect *P. aeruginosa's* ability to survive predation. When taken together, these results suggest that the evolution of *P. aeruginos*a in low nutrient environments selected for strains that were generally better able to reduce amoebae trophozoites levels, either through nutrient sequestration or direct inhibition of the amoebae.

Discussion:

The adaptations that occur in response to long periods without sufficient food sources could impact how bacteria grow (both in terms of how fast and how to divide their limited resources), sense and respond to their environment, their lifestyle, or how they defend themselves against predation. Culturing *P. aeruginosa* for 3 months under low nutrient conditions resulted in alterations to multiple phenotypes associated with fitness and/or virulence. Some of these observed changes in phenotype were shared amongst most of the evolved lineages, regardless of ancestral strain. These changes in phenotypes include faster generation time, reduced cell size, increased pyocyanin production, and decreased motility. Since these phenotypes were observed in most lineages, it could be inferred that these phenotypic alterations lead to increased fitness and thus are likely to occur in these types of environments. Two other phenotypes tested were biofilm formation and pyoverdine production where we observed

variable changes between strains and within replicate evolved lineages within each strain. This indicates that these phenotypes were likely not as strongly selected for in our experimental evolution system [39].

The environments where these particular *P. aeruginosa* strains were isolated likely had higher levels of nutrients (i.e. the clinical isolates) or fluctuating levels of nutrients (household drains). Therefore, the ancestral strains used in our experiments were likely not well adapted to constant low nutrient conditions. Evolved lineages of five of the six strains tested exhibited significantly faster growth compared to their ancestors indicating that the evolved lineages became better adapted to the environment in which they were evolved (Fig. 1). These results are consistent with results observed in other experimental evolution systems such as those observed in the Long-Term Evolution Experiment (LTEE) of *Escherichia coli* where the doubling times of the evolved lineages reduced from 55 minutes to 23 minutes in the minimal nutrient medium used in the experiment after ~50,000 generations [39]. In contrast, the evolved lineages of the mucoid clinical strain, B84725, exhibited significantly increased generation times compared to their ancestor (Fig. 1). While this result was initially puzzling, it is important to consider that the ancestral strain of B84725 is a mucoid variant of *P. aeruginosa.* Mucoid phenotypes are commonly associated with slower generation times and a propensity for biofilm lifestyle in which replication is slowed [40]. It is therefore possible that a slower generation time may have been selected for in this strain. Surprisingly, we did not observe any direct correlation between cell size and generation time suggesting that cell size does not play a factor in doubling time for *P. aeruginosa* as it does for *E. coli* [31], at least not over the short term evolution experiment described here.

Our experimental evolution system theoretically should have strongly selected for increased biofilm formation. Surprisingly, evolved lineages in two of the six strains produced significantly less biofilm biomass than their ancestors while the evolved lineages of the remaining four strains were not significantly different from their ancestors (Fig. 3). One potential explanation for this could be the low-nutrient culture medium used in the evolution experiment. Biofilms require the production and secretion of polysaccharides and extracellular proteins to form the biofilm matrix [41-43]. These matrix components are undoubtedly metabolically costly to produce as the responsibility for exopolysaccharide matrix generation has been shown to be a shared responsibility within a biofilm in other species of bacteria such as *Bacillus subtilis* [44]. Thus, it is possible that the cells either acquired mutations that blocked the biosynthesis or export of some of the necessary biofilms components – perhaps choosing to use the limited carbon for growth rather than EPS production. In addition, the evolved cells used other methods of attachment to the plate surface, such as pili or fimbriae, to avoid the expense of secreting polysaccharides. These structures are typically used in the beginning stages of biofilm attachment prior to EPS production. Thus, *P. aeruginosa* could have attached to the surface but not initiated polysaccharide secretion to save nutrients for growth. While speculatively, this series of events would result in cells with better metabolic fitness in their environment but result in a tradeoff of a reduced ability to form biofilms with large biomass. This result is similar to those observed in *P. aeruginosa* strains co-cultured long-term with the amoebal predator, *A. castellanii,* in a minimal nutrient medium [45]. In this latter study, biofilm biomass was found to decrease in *P. aeruginosa* strains cultured in monoculture as well as in co-culture with *A. castellanii* in minimal media for 42 days.

We expected that flagellar motility would be selected against in our experimental evolution because planktonic cells were removed during every passage. A reduction in motility was observed in the evolved lineages of strains where the ancestors exhibited high motility (Fig. 5). This result is similar to results observed in *P. aeruginosa* PAO1 cultured in artificial CF medium for 120 days under aerated conditions both in monoculture and in the presence of phage competitors [46]. In our study, the evolved lineages of two strains, PA B80427 and PA B84725, did not exhibit a reduction in motility, perhaps because the ancestors were poorly motile/amotile and possibly do not have enough loci for evolution to act upon (*i.e.*, lacking flagella biosynthesis genes).

We also had hypothesized that pyocyanin production would be increased in the evolved populations compared to their ancestors because outside of its toxic effects on host and other prokaryotic cells, pyocyanin serves as a secondary metabolite, stabilizing the redox state of *P. aeruginosa* and can act as a final electron acceptor in the electron transport chain [33]. Increased expression/production of pyocyanin should therefore increase metabolic fitness in low nutrient environments. Pyocyanin has also been shown to play a role in pyruvate excretion and metabolism under anoxic conditions which are common in the lung environment and in biofilms [33-35]. *P. aeruginosa* has been shown to be able to ferment excreted pyruvate to survive in anoxic/low-nutrient conditions for at least 18 days [34]. Our pyocyanin hypothesis was supported for half of the evolved lineages when three of the six strains showed a significant increase in pyocyanin production compared to their ancestors. Because our cultures were static, it could be that increases in pyocyanin were observed for those strains that needed additional electron acceptors for their particular electron transport chain while other strains did not.

In contrast, production of pyoverdine, a siderophore, was not significantly altered in almost all evolved lineages compared to their ancestors. This result indicates that pyoverdine was not selected for or against in our experimental evolution design. This result is in opposition to results observed in previous studies which found that pyoverdine production decreased over the course of 42 days in a minimal nutrient medium [45]. It is possible that the 1% HL5 used in our study contained more freely available iron and thus was not selected for or against in our experimental evolution system compared to the supplemented M9 medium used in the previous study.

In addition to identifying phenotypic changes that occurred in our evolved isolates, we also sought to determine if adaptations to a low nutrient environment could have implications on virulence against host organisms. *A. castellanii* a bacterivorous amoebae species was identified as a model organism to study phagocytosis because of its commonalities with phagocytic human immune cells, such as macrophages [3-6]. Trophozoite survival tended to be higher when co-cultured with the evolved isolates of the other four strains than when in co-culture with the ancestral isolates at 16-days of co-culture (Figs. 8 and S7). However, this result was not consistent when looking at trophozoite survival over time. In most cases, trophozoite mortality was greater when co-cultured with evolved isolates compared to ancestors (Fig. S7). All the evolved lineages of *P. aeruginosa* were just as capable of surviving predation from the amoebae predator as their ancestors were. One potential reason that might underlie why *A. castellanii* trophozoites tended to survive better with the ancestors than with the evolved lineages over time could be due to the reduced motility observed in our evolved lineages. *Campylobacter jejuni*, *Pseudomonas fluorescens*, and *Proteus mirabilis* flagellin has been shown to be recognized by *A. castellanii* to initiate phagocytosis [47, 48]. Thus, if there are fewer/less flagella expressed in the

evolved isolates, there would be less predation by *A. castellanii* resulting in starvation of the amoebae predator when in co-culture with the evolved lineages.

In summary, a variety of *P. aeruginosa* phenotypes were observed to change over the course of long periods with limited resources, but there was a great deal of variability in how *P. aeruginosa* chose to invest its resources based on individual lineage data. This may not be surprising, given the genomic plasticity within *P. aeruginosa* as a species. These results are significant as they contribute to fundamental scientific knowledge into how *P. aeruginosa* might evolve in other low nutrient environments (such as sink drains and faucets, hospital surfaces, or freshwaters). This work could also yield insights into expected changes in *P. aeruginosa* over time in low nutrient environments and this could have implications for virulence properties or treatment efficacy for human infections. Lastly, this work could set the stage for future evolution experiments in which *P. aeruginosa* could be evolved with predators, such as macrophage or amoeba, to examine the effect of nutrient concentration on host-pathogen interactions.

Figure legends:

Figure 1. Relative generation time in 1% HL5 at room temperature. Grey bars represent the ancestors, and the colored bars represent the average of three evolved lineages. Data analyzed with t-tests between ancestor (n=4) and evolved lineages (n=12). Error bars represent standard deviation. * $p<0.05$, *** $p<0.0001$.

Figure 2. Cell size after 3-months in 1% HL5. Grey bars represent average values for isolate of the ancestor strain (n=20) while colored bars represent the average of three evolved isolates

(n=60 total). Data analyzed with t-tests between ancestors and evolved lineages. Error bars represent standard deviation. * $p<0.05$, ** $p<0.01$.

Figure 3. Biofilm biomass of 48-hour biofilms of ancestral and evolved isolates in 1% HL5. Grey bars represent ancestors (n=4), colored bars represent the average of three evolved isolates [n=12 (4 isolates from 3 individual evolved lineages)]. Data analyzed with t-tests between the ancestor and evolved lineages. Error bars represent standard deviation. Ancestor bars n=4, evolved isolate bars n=12 (4 isolates from 3 individual evolved lineages). *** $p<0.005$, **** $p<0.0001$.

Figure 4. Pyocyanin production of 12-week-old evolved lineages compared to ancestors. Grey bars represent ancestors (n=4), colored bars represent the average of three evolved isolates (n=12). Data analyzed with t-tests between the ancestor and evolved lineages. Error bars represent standard deviation. * $p<0.05$, ** $p<0.01$.

Figure 5. Pyoverdine production of ancestor and 12-week-old evolved isolates. Grey bars represent ancestors, colored bars represent the average of three evolved isolates. Data analyzed with t-tests between the ancestor and evolved lineages. Error bars represent standard deviation. Ancestor bars n=4, evolved isolate bars n=12. * $p<0.05$.

Figure 6. Swimming motility of ancestral and evolved isolates in 0.3% LB agar. (A) Ancestral vs evolved isolates at 12 weeks, grey bars represent ancestors, and colored bars represent the average of three evolved isolates. Black hashed line indicates growth at the stab line only or amotile. Data analyzed with t-tests between the ancestor and evolved lineages. Error bars

represent standard deviation. Ancestor bars n=3, evolved isolate bars n=9. * $p<0.05$, ** $p<0.01$, **** $p<0.0001$. (Panels B - E) motility of evolved lineages compared to their ancestor (dashed line) at different time points during the evolution to show when motility was lost for (B) B80398, (C) PA3, (D) 17-047, and (E) 17-05. Data analyzed with one-way ANOVA with Tukey's post-test. Letters represent significant differences.

Figure 7. *Acanthamoeba castellanii* survival in co-culture with ancestor and evolved isolates of 6 *P. aeruginosa* strains over time for 16 days. *A. castellanii* trophozoites were enumerated on days 0, 3, 6, 8, 11, 13, and 16. Data represents the average number of trophozoites counted across all time points. Data analyzed with t-test. Error bars represent standard deviation (n=3). **** $p <0.0001$.

Figure 8. Testing survival/killing potential of ancestral and evolved lineages of *P. aeruginosa* against a model host, *Acanthamoeba castellanii*. Grey bars represent ancestors while colored bars represent evolved lines. (A) *A. castellanii* trophozoite survival after 16 days of co-culture. (B) *P. aeruginosa* survival after 16 days of co-culture. Data analyzed with t-tests between ancestral and evolved isolates. Error bars represent standard deviation (n=3). *** $p<0.0005$, **** $p<0.0001$.

Supplemental figure legends:

Figure S1. Relative generation time of individual evolved lineages compared to their ancestor in 1% HL5 at 22°C. Error bars represent standard deviation from four independent colonies from each lineage chosen randomly from agar plates. Data analyzed with one-way ANOVA with Dunnett's post-test comparing each evolved line to its ancestor. * $p<0.05$, ** $p<0.01$, *** $p<0.001$.

Figure S2. Growth curves of the evolved lineages and their ancestors over 42 hours in 1% HL5 at room temperature. Growth curve lines were generated by spectrophotometer data recorded every 30 minutes for 42 hours. Lines represent the mean of 3 biological replicates. Error bars are not shown for image clarity. Data analyzed with one-way ANOVA with Dunnett's post-test comparing evolved lineages to their ancestor. *** $p<0.001$

Figure S3. Cell size of individual evolved lineages compared to their ancestor after 3-month experimental evolution. Error bars represent standard deviation from four independent colonies from each lineage. Data analyzed with one-way ANOVA with Dunnett's post-test comparing each evolved line to its ancestor. * $p<0.05$, ** $p<0.01$.

Figure S4. Biofilm biomass of individual evolved lineages compared to their ancestor after 3-month experimental evolution. Error bars represent standard deviation from four independent colonies from each lineage. Data analyzed with one-way ANOVA with Dunnett's post test comparing each evolved line to its ancestor.). * $p<0.05$, ** $p<0.01$, *** $p<0.001$.

Figure S5. Pyocyanin production of individual isolates compared to their ancestor after 3-month experimental evolution. Error bars represent standard deviation from three independent colonies from each lineage. Data analyzed with one-way ANOVA with Dunnett's post-test comparing each evolved line to its ancestor. * $p<0.05$, ** $p<0.01$.

Figure S6. Pyoverdine production of individual isolates compared to their ancestor after 3-month experimental evolution. Error bars represent standard deviation from three independent colonies from each lineage. Data analyzed with one-way ANOVA with Dunnett's post-test comparing each evolved line to its ancestor. Error bars indicate standard deviation. ** $p<0.01$.

Figure S7. Swimming motility of individual isolates compared to their ancestor after 3-month experimental evolution. Error bars represent standard deviation from three independent colonies from each lineage. Data analyzed with one-way ANOVA with Dunnett's post-test comparing each evolved line to its ancestor. Error bars indicate standard deviation. * $p<0.05$, ** $p<0.01$, *** $p<0.001$.

Figure S8. Competition assay between the ancestor and evolved lineages of *P. aeruginosa* against *Acanthamoeba castellanii* at all timepoints tested. Grey bars represent ancestor while colored bars represent evolved lineages. Graphs represent *A. castellanii* trophozoite numbers when co-cultured with ancestor and evolved lineage of (A) PA B80398, (B) PA B80427, (C) PA B84725, (D) PA3, (E) SRP 17-047, and (F) SRP 17-055 for 0-,3-,6-,8-,11-,13-, and 16-days. Error bars represent standard deviation from three independent colonies from each lineage. Data analyzed with t-tests between ancestor and evolved lineage at each timepoint. * $p<0.05$, ** $p<0.01$, *** $p<0.001$, **** $p<0.0001$.

References

[1] Ebert D. Experimental Evolution of Parasites. Science (New York, NY). 1998;282:1432-6.

[2] Wong A, Rodrigue N, Kassen R. Genomics of adaptation during experimental evolution of the opportunistic pathogen Pseudomonas aeruginosa. 2012.

[3] Kuburich NA, Adhikari N, Hadwiger JA. Acanthamoeba and Dictyostelium Use Different Foraging Strategies. Protist. 2016;167:511-25.

[4] Kumar A, Molli PR, Pakala SB, Nguyen TMB, Rayala SK, Kumar R. PAK thread from amoeba to mammals. Journal of cellular biochemistry. 2009;107:579-85.

[5] Al-Quadan T, Price CT, Abu Kwaik Y. Exploitation of evolutionarily conserved amoeba and mammalian processes by *Legionella*. Trends Microbiol. 2012;20:299-306.

[6] Siddiqui R, Khan NA. Biology and pathogenesis of Acanthamoeba. Parasit Vectors. 2012;5:6.

[7] Santajit S, Indrawattana N. Mechanisms of Antimicrobial Resistance in ESKAPE Pathogens. Biomed Res Int. 2016;2016:2475067.

[8] Hancock RE, Speert DP. Antibiotic resistance in *Pseudomonas aeruginosa*: mechanisms and impact on treatment. Drug resistance updates. 2000;3:247-55.

[9] Fernández-Billón M, Llambías-Cabot AE, Jordana-Lluch E, Oliver A, Macià MD. Mechanisms of antibiotic resistance in *Pseudomonas aeruginosa* biofilms. Biofilm. 2023:100129.

[10] Botelho J, Tüffers L, Fuss J, Buchholz F, Utpatel C, Klockgether J, et al. Phylogroup-specific variation shapes the clustering of antimicrobial resistance genes and defence systems across regions of genome plasticity in *Pseudomonas aeruginosa*. EBioMedicine. 2023;90.

[11] Mendes OR. The challenge of pulmonary *Pseudomonas aeruginosa* infection: How to bridge research and clinical pathology. Viral, Parasitic, Bacterial, and Fungal Infections: Elsevier; 2023. p. 591-608.

[12] Walker TS, Bais HP, Déziel E, Schweizer HP, Rahme LG, Fall R, et al. *Pseudomonas aeruginosa*-plant root interactions. Pathogenicity, biofilm formation, and root exudation. Plant physiology. 2004;134:320-31.

[13] Hou L, Debru A, Chen Q, Bao Q, Li K. AmrZ regulates swarming motility through cyclic di-GMP-dependent motility inhibition and controlling Pel polysaccharide production in *Pseudomonas aeruginosa* PA14. Frontiers in microbiology. 2019;10:1847.

[14] Coggan KA, Wolfgang MC. Global regulatory pathways and cross-talk control *Pseudomonas aeruginosa* environmental lifestyle and virulence phenotype. Current issues in molecular biology. 2012;14:47-70.

[15] Hall CL, Lee VT. Cyclic□di□GMP regulation of virulence in bacterial pathogens. Wiley Interdisciplinary Reviews: RNA. 2018;9:e1454.

[16] Römling U, Galperin MY, Gomelsky M. Cyclic di-GMP: the first 25 years of a universal bacterial second messenger. Microbiol Mol Biol Rev. 2013;77:1-52.

[17] Matz C, Moreno AM, Alhede M, Manefield M, Hauser AR, Givskov M, et al. *Pseudomonas aeruginosa* uses type III secretion system to kill biofilm-associated amoebae. The ISME journal. 2008;2:843-52.

[18] Johns BE, Purdy KJ, Tucker NP, Maddocks SE. Phenotypic and genotypic characteristics of small colony variants and their role in chronic infection. Microbiology insights. 2015;8:MBI. S25800.

[19] Thi MTT, Wibowo D, Rehm BHA. *Pseudomonas aeruginosa* Biofilms. International Journal of Molecular Sciences. 2020;21:8671.

[20] Britigan BE, Roeder TL, Rasmussen GT, Shasby DM, McCormick ML, Cox CD. Interaction of the *Pseudomonas aeruginosa* secretory products pyocyanin and pyochelin generates hydroxyl radical and causes synergistic damage to endothelial cells. Implications for *Pseudomonas*-associated tissue injury. J Clin Invest. 1992;90:2187-96.

[21] Hauser AR. The type III secretion system of *Pseudomonas aeruginosa*: infection by injection. Nature Reviews Microbiology. 2009;7:654-65.

[22] Cecil RE, Yoder-Himes DR. Examining the influence of environmental factors on *Acanthamoeba castellanii* and *Pseudomonas aeruginosa* in co-culture. bioRxiv. 2024:2024.01. 17.575952.

[23] Merritt JH, Kadouri DE, O'Toole GA. Growing and analyzing static biofilms. Current protocols in microbiology. 2011;22:1B. .-B. .18.

[24] Gajdács M, Baráth Z, Kárpáti K, Szabó D, Usai D, Zanetti S, et al. No correlation between biofilm formation, virulence factors, and antibiotic resistance in *Pseudomonas aeruginosa*: results from a laboratory-based in vitro study. Antibiotics. 2021;10:1134.

[25] Remold SK, Brown CK, Farris JE, Hundley TC, Perpich JA, Purdy ME. Differential habitat use and niche partitioning by *Pseudomonas* species in human homes. Microbial ecology. 2011;62:505-17.

[26] Purdy-Gibson M, France M, Hundley T, Eid N, Remold S. *Pseudomonas aeruginosa* in CF and non-CF homes is found predominantly in drains. Journal of Cystic Fibrosis. 2015;14:341-6.

[27] Mojesky AA, Remold SK. Spatial structure maintains diversity of pyocin inhibition in household *Pseudomonas aeruginosa*. Proceedings of the Royal Society B. 2020;287:20201706.

[28] Ramsey DM, Wozniak DJ. Understanding the control of *Pseudomonas aeruginosa* alginate synthesis and the prospects for management of chronic infections in cystic fibrosis. Molecular microbiology. 2005;56:309-22.

[29] LaBauve AE, Wargo MJ. Growth and laboratory maintenance of *Pseudomonas aeruginosa*. Current protocols in microbiology. 2012;25:6E. 1.-6E. 1.8.

[30] Eagon RG. *Pseudomonas natriegens*, a marine bacterium with a generation time of less than 10 minutes. Journal of bacteriology. 1962;83:736-7.

[31] Westfall CS, Levin PA. Bacterial cell size: multifactorial and multifaceted. Annual review of microbiology. 2017;71:499-517.

[32] Wang JD, Levin PA. Metabolism, cell growth and the bacterial cell cycle. Nature reviews Microbiology. 2009;7:822-7.

[33] Price-Whelan A, Dietrich LE, Newman DK. Pyocyanin alters redox homeostasis and carbon flux through central metabolic pathways in *Pseudomonas aeruginosa* PA14. J Bacteriol. 2007;189:6372-81.

[34] Eschbach M, Schreiber K, Trunk K, Buer J, Jahn D, Schobert M. Long-term anaerobic survival of the opportunistic pathogen *Pseudomonas aeruginosa* via pyruvate fermentation. Journal of bacteriology. 2004;186:4596-604.

[35] Costa KC, Glasser NR, Conway SJ, Newman DK. Pyocyanin degradation by a tautomerizing demethylase inhibits *Pseudomonas aeruginosa* biofilms. Science. 2017;355:170-3.

[36] Cox CD, Adams P. Siderophore activity of pyoverdin for *Pseudomonas aeruginosa.* Infection and immunity. 1985;48:130-8.

[37] Jeong G-J, Khan F, Khan S, Tabassum N, Mehta S, Kim Y-M. *Pseudomonas aeruginosa* virulence attenuation by inhibiting siderophore functions. Applied Microbiology and Biotechnology. 2023;107:1019-38.

[38] Siddiqui R, Khan NA. Biology and pathogenesis of *Acanthamoeba*. Parasites & vectors. 2012;5:1-13.

[39] Lenski RE. Experimental evolution and the dynamics of adaptation and genome evolution in microbial populations. The ISME journal. 2017;11:2181-94.

[40] Yang L, Haagensen JA, Jelsbak L, Johansen HK, Sternberg C, Høiby N, et al. *In situ* growth rates and biofilm development of *Pseudomonas aeruginosa* populations in chronic lung infections. Am Soc Microbiol; 2008.

[41] Ma L, Conover M, Lu H, Parsek MR, Bayles K, Wozniak DJ. Assembly and development of the *Pseudomonas aeruginosa* biofilm matrix. PLoS pathogens. 2009;5:e1000354.

[42] Ryder C, Byrd M, Wozniak DJ. Role of polysaccharides in *Pseudomonas aeruginosa* biofilm development. Current opinion in microbiology. 2007;10:644-8.

[43] Toyofuku M, Roschitzki B, Riedel K, Eberl L. Identification of proteins associated with the *Pseudomonas aeruginosa* biofilm extracellular matrix. Journal of proteome research. 2012;11:4906-15.

[44] York A. Sharing the burden to build a matrix. Nature Reviews Microbiology. 2018;16:454-5.

[45] Leong W, Lutz C, Williams J, Poh YH, Yee BYK, Chua C, et al. *Pseudomonas aeruginosa* isolates co-incubated with *Acanthamoeba castellanii* exhibit phenotypes similar to chronic cystic fibrosis isolates. bioRxiv. 2020:2020.02. 25.964320.

[46] Davies EV, James CE, Brockhurst MA, Winstanley C. Evolutionary diversification of *Pseudomonas aeruginosa* in an artificial sputum model. BMC microbiology. 2017;17:1-10.

[47] Nasher F, Wren BW. Flagellin O-linked glycans are required for the interactions between *Campylobacter jejuni* and *Acanthamoebae castellanii*. Microbiology. 2023;169:001386.

[48] Preston T, King C. Binding sites for bacterial flagella at the surface of the soil amoeba *Acanthamoeba*. Microbiology. 1984;130:1449-58.

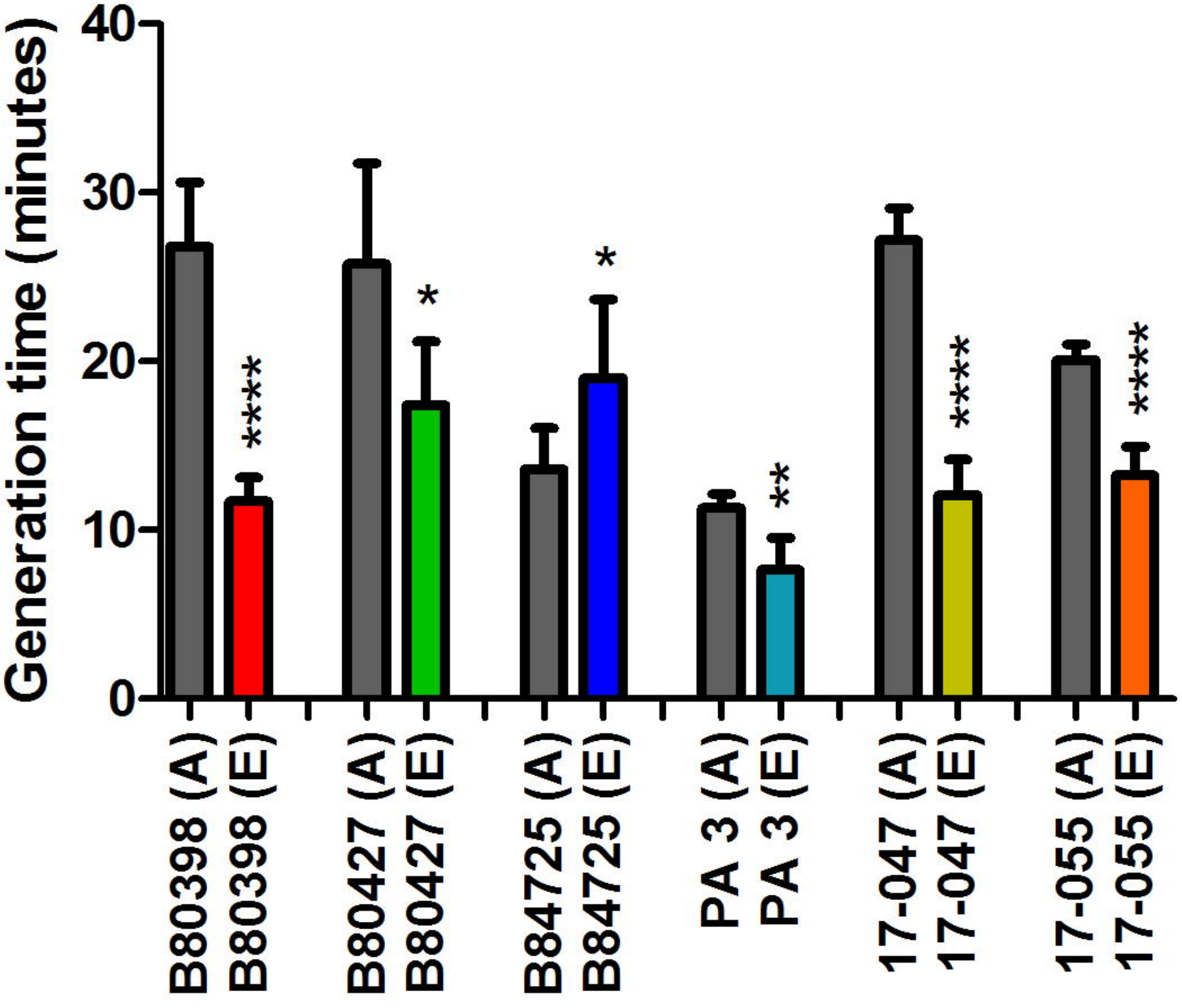
Generation time (minutes)
40
30
20
10
0
****
*
*
**
****
****
B80398 (A)
B80398 (E)
B80427 (A)
B80427 (E)
B84725 (A)
B84725 (E)
PA 3 (A)
PA 3 (E)
17-047 (A)
17-047 (E)
17-055 (A)
17-055 (E)

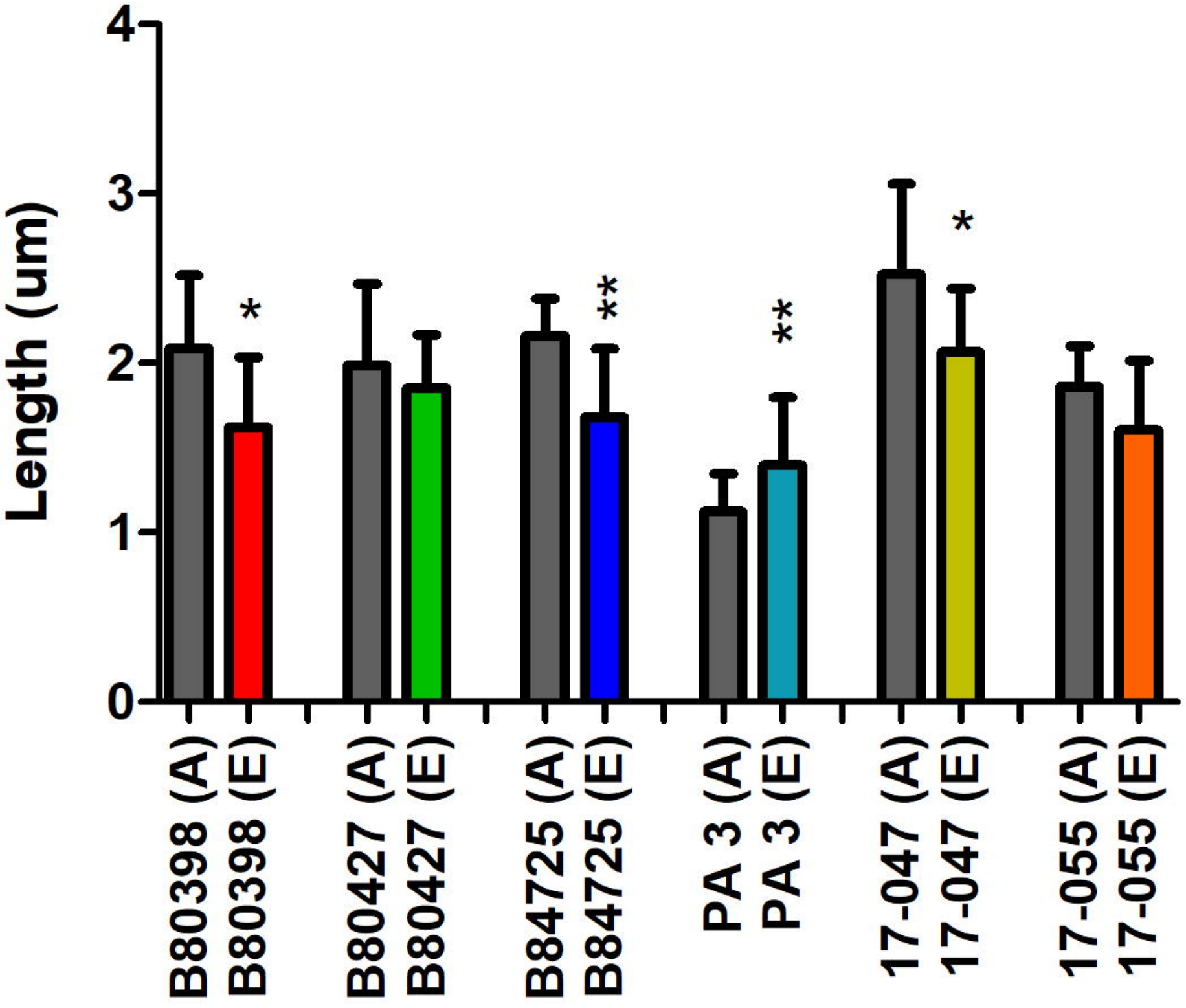
Length (um)
4
3
2
1
0
*
**
**
*
B80398 (A)
B80398 (E)
B80427 (A)
B80427 (E)
B84725 (A)
B84725 (E)
PA 3 (A)
PA 3 (E)
17-047 (A)
17-047 (E)
17-055 (A)
17-055 (E)

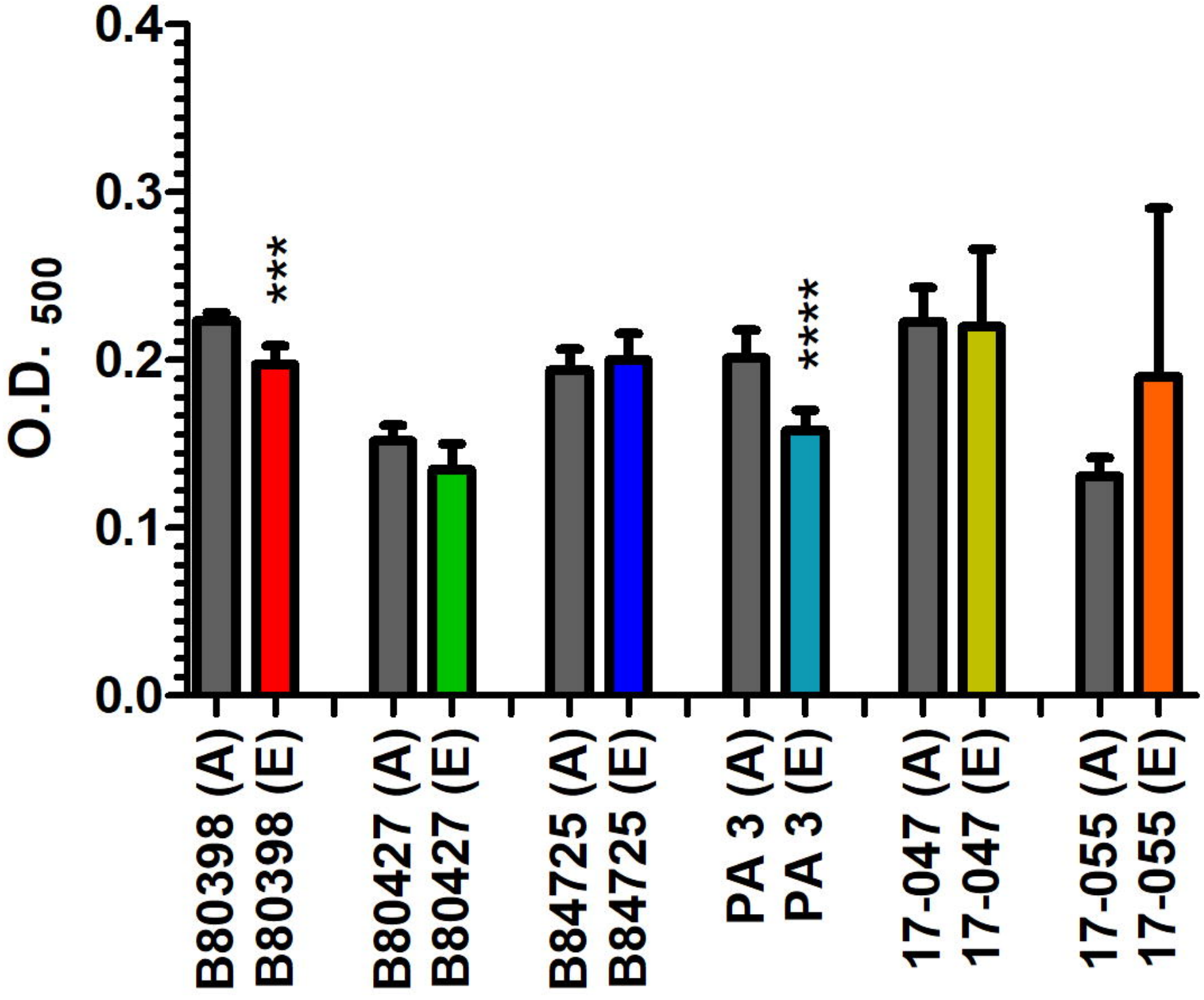
O.D. 500
0.4
0.3
0.2
0.1
0.0
***
****
B80398 (A)
B80398 (E)
B80427 (A)
B80427 (E)
B84725 (A)
B84725 (E)
PA 3 (A)
PA 3 (E)
17-047 (A)
17-047 (E)
17-055 (A)
17-055 (E)

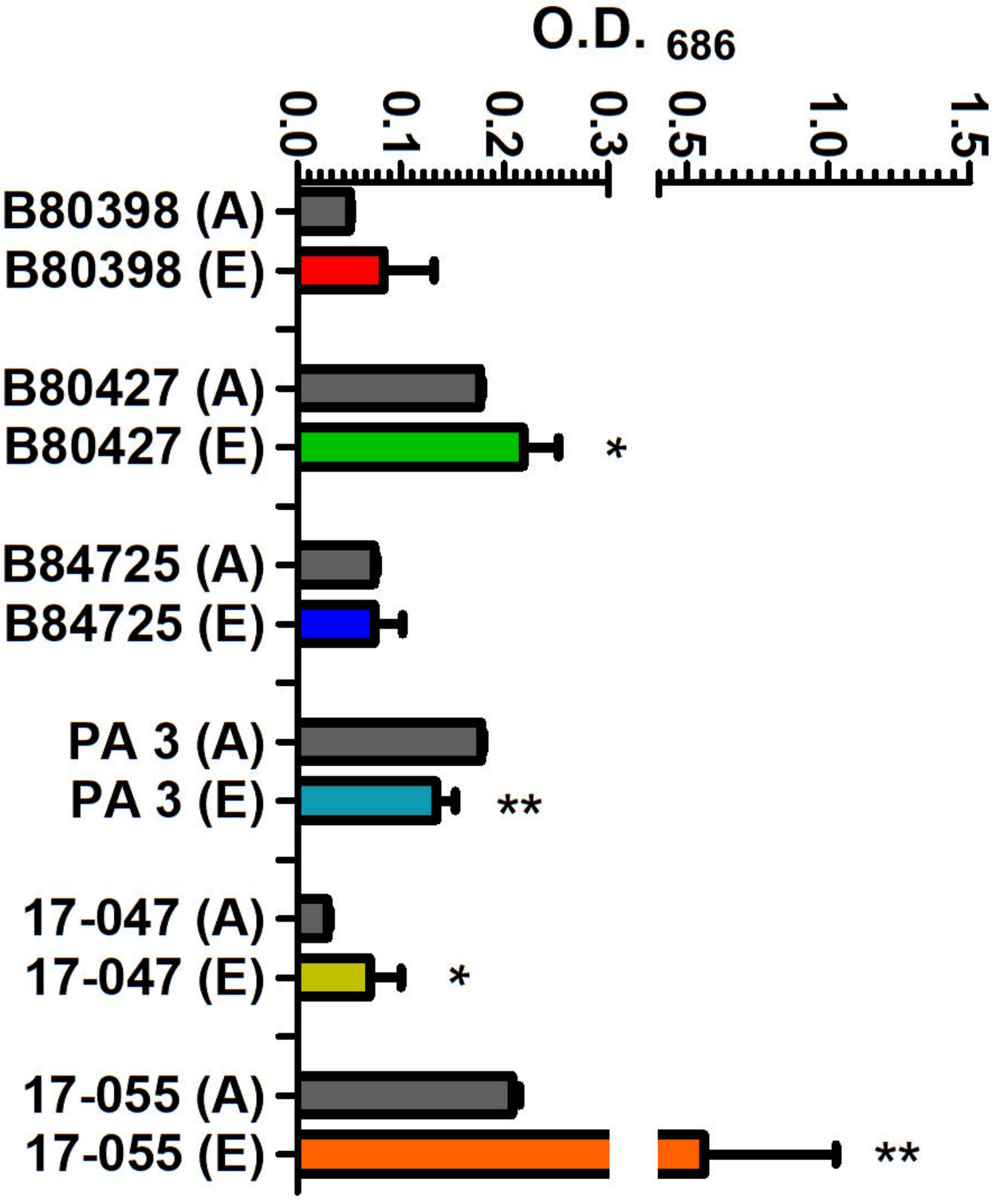
O.D. 686
0.0
0.1
0.2
0.3
0.5
1.0
1.5
B80398 (A)
B80398 (E)
B80427 (A)
B80427 (E)
*
B84725 (A)
B84725 (E)
PA 3 (A)
PA 3 (E)
**
17-047 (A)
17-047 (E)
*
17-055 (A)
17-055 (E)
**

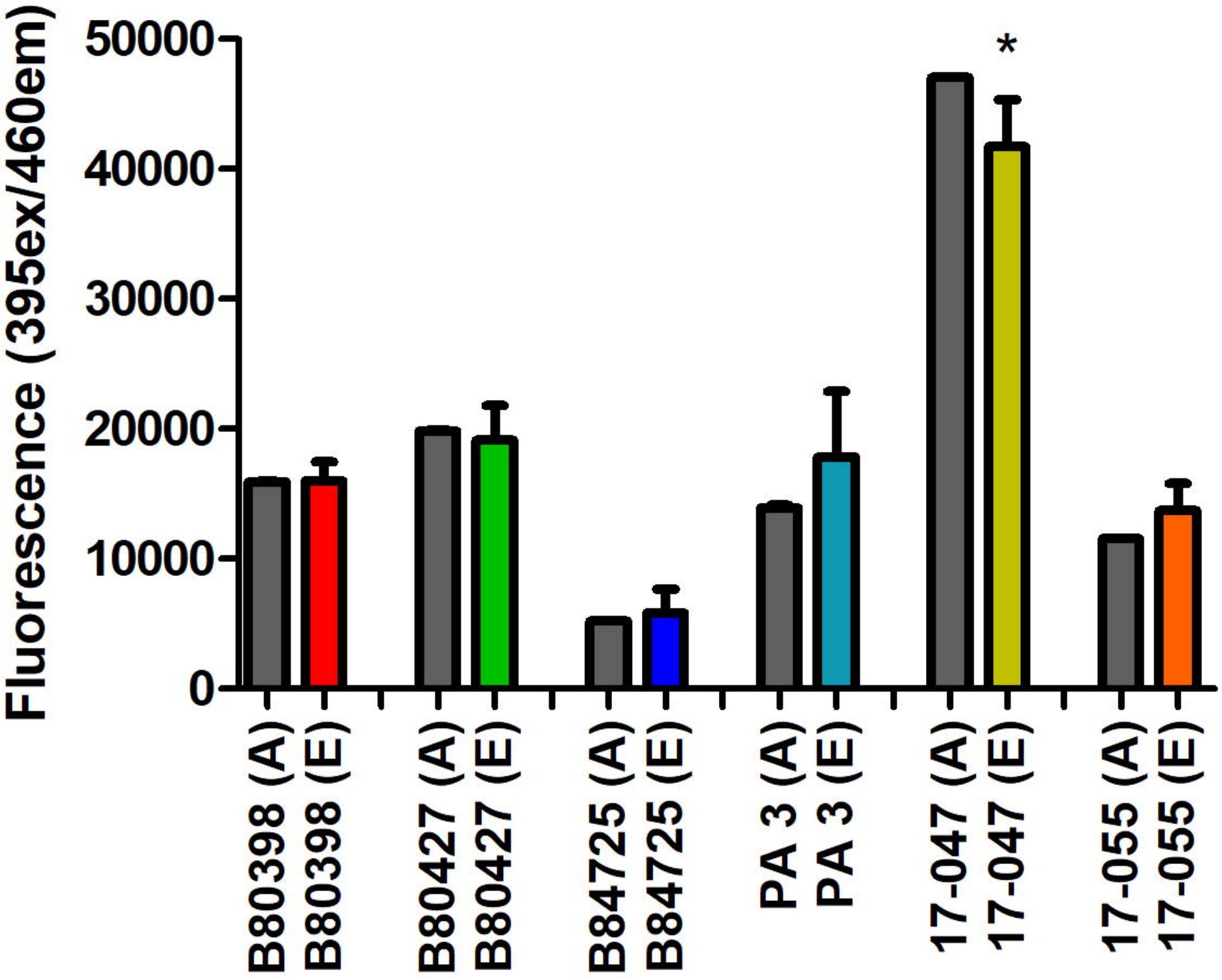
Fluorescence (395ex/460em)
50000
40000
30000
20000
10000
0
*
B803398 (A)
B803398 (E)
B804427 (A)
B804427 (E)
B84725 (A)
B84725 (E)
PA 3 (A)
PA 3 (E)
17-047 (A)
17-047 (E)
17-055 (A)
17-055 (E)

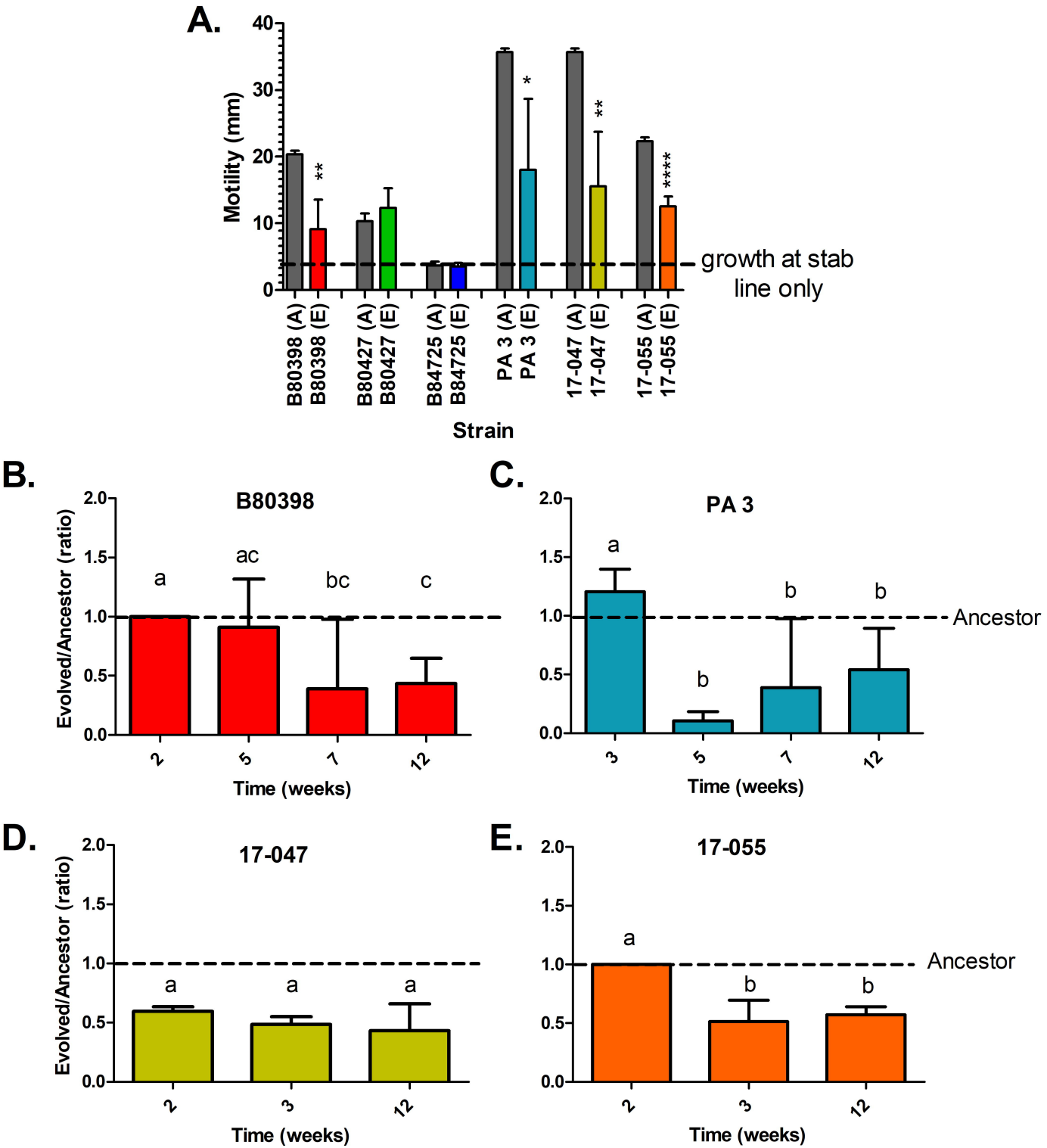
A.
Motility (mm)
40
30
20
10
0
**
*
**
****
growth at stab line only
B80398 (A)
B80398 (E)
B80427 (A)
B80427 (E)
B84725 (A)
B84725 (E)
PA 3 (A)
PA 3 (E)
17-047 (A)
17-047 (E)
17-055 (A)
17-055 (E)
Strain
B.
B80398
Evolved/Ancestor (ratio)
2.0
1.5
1.0
0.5
0.0
a
ac
bc
c
2
5
7
12
Time (weeks)
C.
PA 3
a
b
b
b
Ancestor
3
5
7
12
Time (weeks)
D.
17-047
a
a
a
2
3
12
Time (weeks)
E.
17-055
a
b
b
Ancestor
2
3
12
Time (weeks)

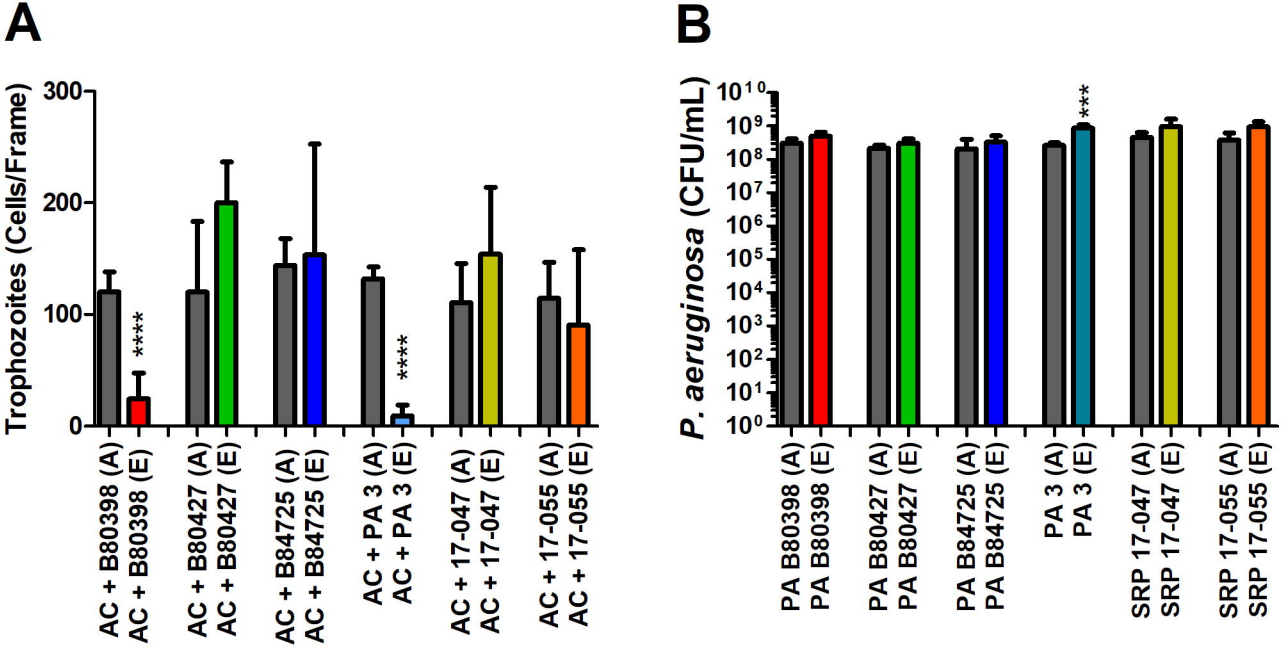
A
Trophozoites (Cells/Frame)
300
200
100
0
****
****
AC + B80398 (A)
AC + B80398 (E)
AC + B80427 (A)
AC + B80427 (E)
AC + B84725 (A)
AC + B84725 (E)
AC + PA 3 (A)
AC + PA 3 (E)
AC + 17-047 (A)
AC + 17-047 (E)
AC + 17-055 (A)
AC + 17-055 (E)
B
P. aeruginosa (CFU/mL)
10^{10}
10^{9}
10^{8}
10^{7}
10^{6}
10^{5}
10^{4}
10^{3}
10^{2}
10^{1}
10^{0}
***
PA B80398 (A)
PA B80398 (E)
PA B80427 (A)
PA B80427 (E)
PA B84725 (A)
PA B84725 (E)
PA 3 (A)
PA 3 (E)
SRP 17-047 (A)
SRP 17-047 (E)
SRP 17-055 (A)
SRP 17-055 (E)

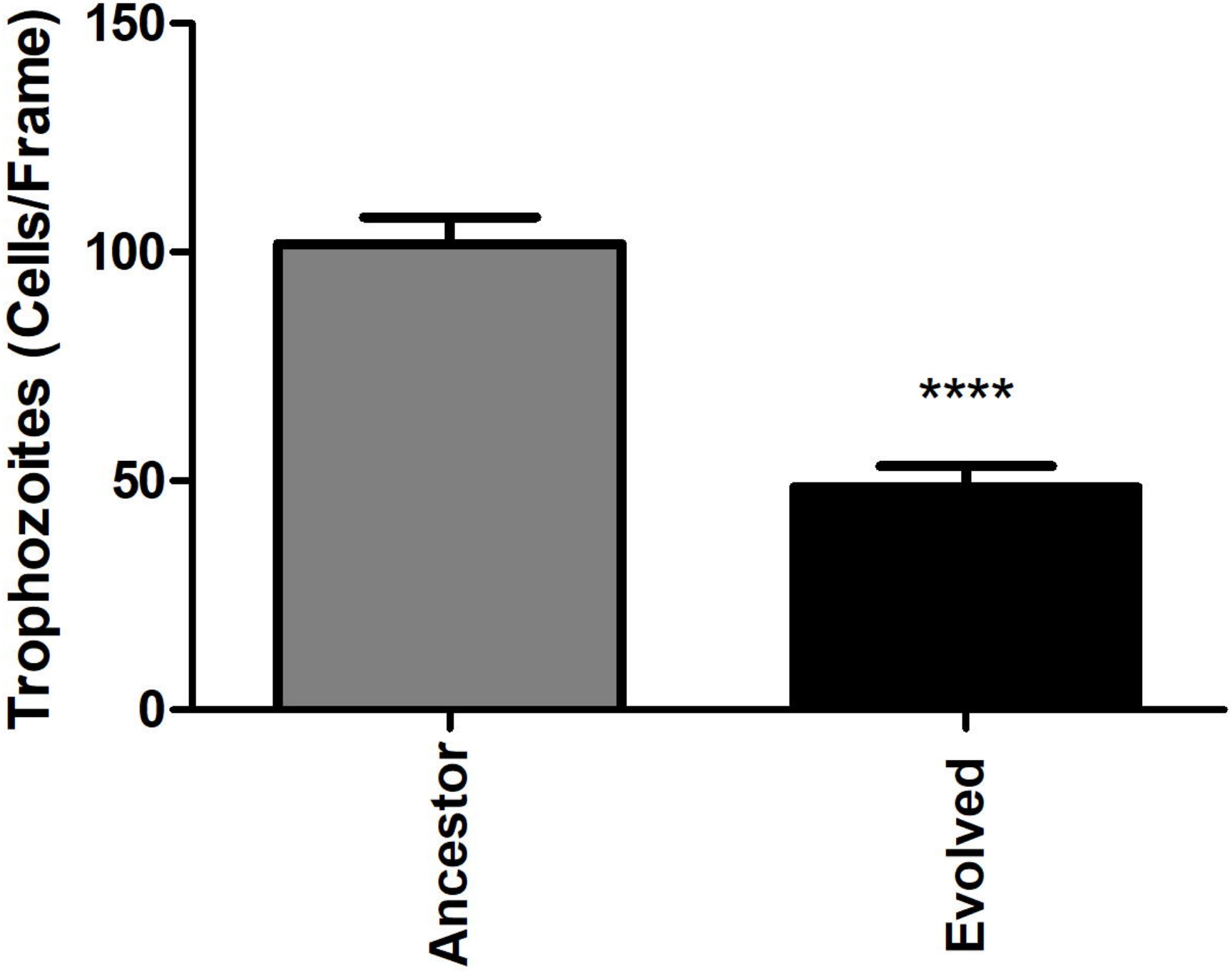
Trophozoites (Cells/Frame)
150
100
50
0
****
Ancestor
Evolved